Eur Radiol (2002) 12:1557–1566
DOI 10.1007/s00330-001-1270-5

Heike E. Daldrup-Link
Ernst J. Rummeny
Bettina Ihssen
Joachim Kienast
Thomas M. Link

Iron-oxide-enhanced MR imaging of bone marrow in patients with non-Hodgkin's lymphoma: differentiation between tumor infiltration and hypercellular bone marrow

Received: 14 August 2001
Revised: 16 September 2001
Accepted: 22 November 2001
Published online: 5 February 2002

This work was presented at ECR 2001

H.E. Daldrup-Link (✉) · E.J. Rummeny
T.M. Link
Department of Radiology,
Technical University of Munich,
Ismaninger Strasse 22, 81675 Munich,
Germany
e-mail: daldrup@roe.med.tu-muenchen.de
Tel.: +49-89-41402621
Fax: +49-89-41402637

B. Ihssen
Department of Radiology,
University of Münster, Münster, Germany

J. Kienast
Department of Oncology,
University of Münster, Münster, Germany

Abstract The aim of this study was to differentiate normal, hypercellular, and neoplastic bone marrow based on its MR enhancement after intravenous administration of superparamagnetic iron oxides in patients with cancer of the hematopoietic system. Eighteen patients with cancer of the hematopoietic system underwent MRI of the spine before and after infusion of ferumoxides (n=9) and ferumoxtran (n=9) using T1- and T2-weighted turbo spin-echo (TSE) and short tau inversion recovery sequences (STIR). In all patients diffuse or multifocal bone marrow infiltration was suspected, based on iliac crest biopsy and imaging such as conventional radiographs, MRI, and positron emission tomography. In addition, all patients had a therapy-induced normocellular (n=7) or hypercellular (n=11) reconversion of the normal non-neoplastic bone marrow. The MRI data were analyzed by measuring pre- and post-contrast signal intensities (SI) of hematopoietic and neoplastic marrow and by calculating the enhancement as ΔSI(%) data and the tumor-to-bone-marrow contrast as contrast-to-noise ratios (CNR). Changes in bone marrow signal intensity after iron oxide administration were more pronounced on STIR images as compared with T1- and T2-weighted TSE images. The STIR images showed a strong signal decline of normal and hypercellular marrow 45–60 min after iron oxide infusion, but no or only a minor signal decline of neoplastic bone marrow lesions; thus, ΔSI% data were significantly higher in normal and hypercellular reconverted marrow compared with neoplastic bone marrow lesions (p<0.05). Additionally, the contrast between focal or multifocal neoplastic bone marrow infiltration and normal bone marrow, quantified by CNR data, increased significantly on post-contrast STIR images compared with precontrast images (p<0.05). Superparamagnetic iron oxides are taken up by normal and hypercellular reconverted bone marrow, but not by neoplastic bone marrow lesions, thereby providing significantly different enhancement patterns on T2-weighted MR images; thus, superparamagnetic iron oxides are useful to differentiate normal and neoplastic bone marrow and to increase the bone marrow-to-tumor contrast.

Keywords MR contrast agents · Ferumoxides · Ferumoxtran · Bone marrow

Introduction

In patients with cancer of the hematopoietic system the diagnosis of neoplastic bone marrow infiltration is crucial to determine prognosis and to identify suitable treatment protocols [1]. Iliac crest biopsy is mandatory for staging and histopathologic classification of the disease [1, 2, 3]. In non-Hodgkin's lymphoma (NHL) a neoplastic bone marrow infiltration indicates the highest stage (stage four) according to the Ann Arbor Classification [1]. In cases of plasmacytoma, the extent of bone marrow infiltration is graded as stage one to three according to the Salmon and Durie classification [1]. In both instances, iliac crest biopsy may be false negative when the bone marrow infiltration is focal rather than diffuse [2, 3]. Magnetic resonance imaging, which may depict a large portion of the entire skeleton, provides important additional information for the diagnosis of neoplastic bone marrow infiltration. Various studies have demonstrated that MR has a high sensitivity for the detection of early bone marrow infiltration, and that patients with bone marrow infiltration on conventional MRI, but negative bone marrow biopsy, have a worse prognosis than patients with both, negative MRI and negative bone marrow biopsy [4, 5, 6].

Special diagnostic problems occur in patients with cancer of the hematopoietic system during therapy. The normal bone marrow undergoes a conversion from highly cellular to fatty marrow with increasing age [7, 8, 9, 10]. In patients with tumor infiltration of the bone marrow prior to therapy, the fatty converted marrow and the highly cellular neoplastic lesions can be differentiated on conventional MR images due to different T1- and T2-relaxation times [8, 11]. After chemotherapy, however, the normal bone marrow may undergo a reconversion from fatty to cellular hematopoietic marrow. In patients with lymphoma, this process may be enhanced by administration of granulocyte colony stimulating factor (GCSF), which activates the hematopoietic marrow and decreases the period of aplasia after chemotherapy. The differentiation between this reconverted hematopoietic marrow and recurrent tumor after chemotherapy is not possible with conventional MR techniques, since relaxation rates and MR signal characteristics of highly cellular hematopoietic and highly cellular neoplastic bone marrow are similar [12]. Various investigators have addressed this problem, but were not able to differentiate reconverted hypercellular hematopoietic marrow and tumor infiltration using a variety of pulse sequences, extracellular contrast agents, and MR spectroscopy [13, 14, 15].

A new approach to this diagnostic dilemma may be the application of iron-oxide-based MR contrast agents. Superparamagnetic iron oxides are phagocytosed by cells of the reticuloendothelial system (RES) in the hematopoietic marrow but are not taken up by neoplastic bone marrow [16, 17]; thus, they may be suited to differentiate hematopoietic marrow and bone marrow tumors. To our knowledge, the potential and limitations of iron oxides in the detection of bone marrow infiltration due to NHL and in the differentiation from reconverted hematopoietic marrow and tumor have not been assessed yet. The goal of this study was therefore to assess the performance of iron-oxide-enhanced MRI in targeting normal hematopoietic bone marrow, in detecting bone marrow infiltration of the spine in patients with lymphoma, and in differentiating between hypercellular hematopoietic marrow and tumor infiltration.

Materials and methods

Patients

Eighteen patients with NHL (11 men and 7 women; age range 37–69 years, mean age 55.3 years) underwent MRI of the spine before and after iron oxide administration in accordance with the regulations of the Committee of Human Research at our institution. Informed consent was obtained from all patients after the nature of the examinations had been fully explained. Pathologic diagnoses included plasmocytoma (stage I, *n*=3; stage II, *n*=1; stage III, *n*=8) according to Salmon and Durie) and other NHL (stage IV, n=6, according to the Ann Arbor Classification). Patients were examined during or after chemotherapy. Inclusion criteria were suspected neoplastic bone marrow infiltration of the axial skeleton, diagnosed by iliac crest biopsy (*n*=16) or imaging modalities, such as MRI (*n*=3), FDG-PET (*n*=2), skeletal scintigraphy (*n*=2), CT (*n*=2), and conventional radiography (*n*=3). Additional inclusion criteria included suspected reconversion of the normal bone marrow because of previous GCSF treatment (*n*=9) and/or signal changes on plain MR images (*n*=18), i.e., low signal intensity relative to the paravertebral muscle on plain T1-weighted images and high signal intensity relative to the paravertebral muscle on plain short tau inversion recovery (STIR) images. The following exclusion criteria were defined: an age of less than 18 years, standard MR contraindications (intracorporal metal devices, e.g., pacemaker, intracranial clips), a history of serious adverse events to contrast agents, iron compounds or other drugs as well as pregnancy and breast feeding. Patients with hemosiderosis, liver cirrhosis, or other diseases with serious liver dysfunction (Child's C) were also excluded. Patients were randomly divided into two groups: 9 patients received superparamagnetic iron oxides (SPIO, ferumoxides), and 9 patients received ultra small SPIO (USPIO, ferumoxtran). Age distribution and mean age were not significantly different between patients treated with ferumoxides (age range 41–67 years, mean age 53.8 years) or ferumoxtran (42–69 years, mean age 56.9 years). During and after contrast agent administration, blood pressure and pulse were monitored and the patients were asked about subjective side effects.

Contrast medium

Ferumoxides (Endorem®, Laboratoire Guerbet, Aulnay-sous-Bois, France) are colloid based superparamagnetic iron oxide particles with an R2/R1 relaxivity ratio ($L \times mmol^{-1}\ s^{-1}$) of 160/40 [18]. Ferumoxides represent Fe_2O_3 and Fe_3O_4 particles with a range in diameter of 120–180 nm, the mean particle diameter is 150 nm. They consist of nonstoichiometric magnetic crystalline cores, which are covered with a ~3.3-nm-thick dextran T-10 layer [18, 19]. Further physical and magnetic characteristics have been described elsewhere [20, 21, 22]. Blood pool half-life was reported to be 20 min

in humans [21]. Ferumoxides were investigated in phase I–III studies as RES-specific contrast agents for the detection and characterization of liver neoplasms and were approved for clinical use in 1994. For this study, ferumoxides were supplied as a solution with a concentration of 11.2 mg iron/ml and 7.6 mg dextran/ml. A dose of 15 µmol Fe/kg body weight (0.84 mg/kg or 0.075 ml/kg), as recommended for clinical applications, was diluted in 100 ml of 5% glucose and slowly infused intravenously through a 0.22-µm filter over 30 min. In 1 patient with diabetes mellitus, ferumoxides were diluted in 100 ml 0.9% saline instead of glucose solution.

Ferumoxtran is a prototype colloid-based ultra-small superparamagnetic iron oxide (Sinerem®, Laboratoire Guerbet, Aulnay-sous-Bois, France), also representing Fe_2O_3 and Fe_3O_4 particles with a dextran layer [19]; however, the particle diameter of 20–50 nm (mean 35 nm) is approximately four times smaller compared with ferumoxides. The R1 relaxivity (37°C, 0.47 T) of 21.6 mmol/kg is considerably shorter and the R2 relaxivity (37°C, 0.47 T) of 44.1 mmol/kg is slightly longer as compared with ferumoxides [23]. Further characteristics of ferumoxtran were described by Jung [19], Weissleder et al. [20], and Chambon et al. [24]. Blood pool half-life was reported to be 24 h in humans [24]. Ferumoxtran was initially used in phase I–III studies as an RES-specific contrast agent for the lymphatic system and as a blood pool agent for MR angiography [23, 25, 26, 27]. For this study, ferumoxtran was supplied as a lyophilized powder and was reconstituted with 10 ml of 0.9% saline to yield a solution containing 20 mg Fe/ml and 57 mg dextran/g. The recommended dose of 30 µmol Fe/kg b.w. (2.6 mg/kg or 0.13 ml/kg) was diluted in 100 ml NaCl 0.9% and infused intravenously through a 0.22-µm filter over 30 min.

MR imaging

Magnetic resonance imaging was performed using a 1.5-T system (Magnetom Vision, Siemens, Erlangen, Germany). The patients were placed supine on a spine surface coil with selective receive modi for the cervical, thoracic, or lumbar spine. Pre-contrast scans were obtained in 5 patients 24 h before and in 13 patients directly before contrast agent administration. Post-contrast imaging was started 45–60 min after the start of the iron oxide infusion. Based on the location of the bone marrow lesions, diagnosed with the initial imaging studies described above, the lumbar and lower thoracic spine were imaged in 12 patients and the thoracic and cervical spine in 6 patients. Pulse sequences comprised sagittal T1-weighted turbo spin echo (TSE; TR/TE=600 ms/15 ms), T2-weighted TSE (TR/TE=4600 ms/90 ms), and short STIR (TR/TE=5500 ms/120 ms) sequences with a slice thickness of 4 mm, an interslice gap of 0.4 mm, a field of view (FOV) of 300–400 mm², and a matrix of 384×512 pixels.

Data analysis

For quantitative data analysis, the signal intensities (SI) of normal bone marrow (not applicable in diffuse bone marrow infiltration), focal and diffuse bone marrow lesions, and background noise were measured by a single observer (B.I.) with operator-defined regions of interest (ROIs) in an anatomical area as large as possible. The enhancement of the normal bone marrow, reconverted bone marrow, and bone marrow lesions was quantified as relative changes in signal intensities (ΔSI (%)), i.e., the difference between pre-contrast tissue signal intensity (SI_{pre}) and post-contrast signal intensity (SI_{post}), normalized by pre-contrast signal intensity:

$$\Delta SI\,(\%) = \left|\left[\left(SI_{post} - SI_{pre}\right)/SI_{pre}\right] \times 100\%\right| .$$

The contrast between the signal intensity (SI) of a focal bone marrow lesion and adjacent normal bone marrow was quantified as the contrast-to-noise ratio (CNR):

$$\mathrm{CNR} = \mathrm{SI}_{\mathrm{lesion}} - \mathrm{SI}_{\mathrm{bonemarrow}}/\mathrm{backgroundnoise} .$$

As a standard of reference for lesion pathology, we used the iliac crest bone marrow aspiration (n=17) and vertebral tumor biopsy (n=1). In addition, a clinical follow-up was obtained 1 year after completion of the study. All other additional imaging modalities, such as MRI with Gd-DTPA (n=4), conventional radiography (n=18), CT (n=5), skeletal scintigraphy (n=6), or FDG-PET (n=4), performed within 2–3 weeks before or after the study, were also assessed.

Statistical analysis

Enhancement data were presented as means and standard errors of the means. To compare differences in ΔSI(%) data for the individual pulse sequences and CNR data pre- and post-contrast, an analysis of variance for repeated measurements was used. Mean data were compared using the Scheffe's test. Statistical significance was assigned for $p<0.05$. All statistical computations were processed using Statview 4.1 software (Abacus, Berkeley, Calif.).

Results

Histopathology from iliac crest aspiration and biopsy showed focal and multifocal disease in 12 patients, diffuse disease in 4 patients, and normal hematopoietic bone marrow without tumor infiltration in 2 patients (Table 1). All patients had either normocellular (n=7) or hypercellular (n=11) bone marrow, and no patient showed fatty marrow conversion. After GCSF treatment, all patients had hypercellular marrow. The relative infiltration of the bone marrow by tumor cells for each patient is shown in Table 1.

No drug-related side effects were observed after ferumoxides or ferumoxtran administration, and the infusion was not interrupted in any of the patients. Four patients had back pain before start of the MR study, and 6 patients complained of increased back pain after completion of the MR study. None of these patients reported increased back pain during contrast agent infusion or release of symptoms directly after the contrast medium infusion.

Hematopoietic bone marrow

After iron oxide infusion, the hematopoietic bone marrow demonstrated no visible changes in signal intensity on T1-weighted images, but a decrease in signal intensity on T2-weighted TSE and STIR images (Table 2). The iron-oxide-induced decrease in bone marrow signal intensity was most pronounced on STIR images and higher after infusion of ferumoxtran as compared with ferumoxides (Fig. 1). ΔSI(%) values were significantly higher using ferumoxtran as compared with ferumoxides for T2-weighted TSE- and STIR sequences ($p<0.05$; Table 2). With both iron oxide contrast agents, the negative bone marrow enhancement on T2-weighted images increased with increasing bone marrow cellularity: The hypercellu-

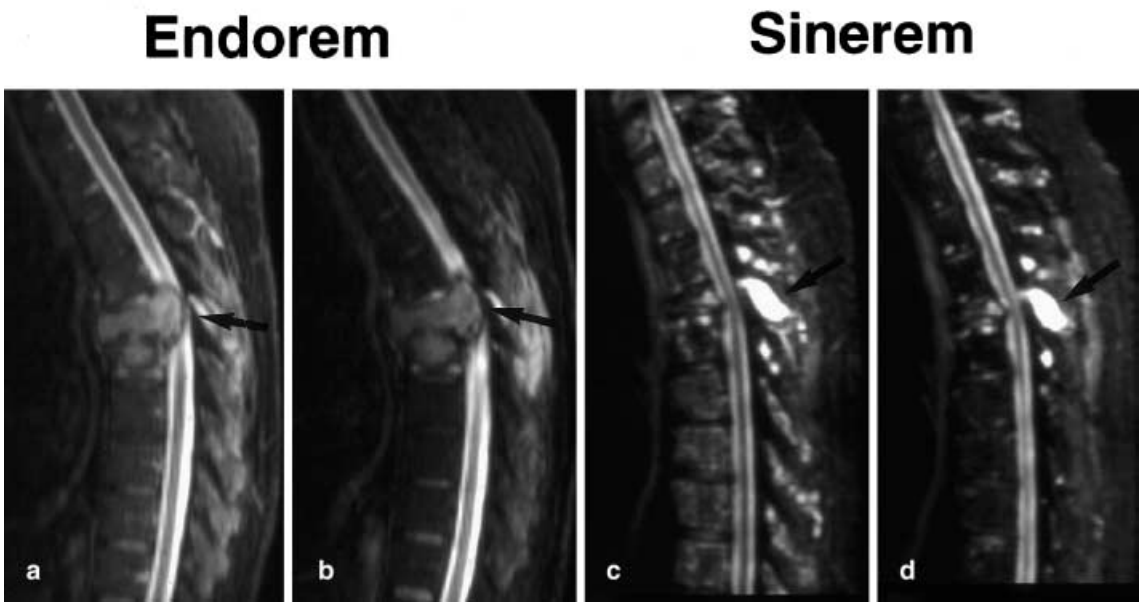

Fig. 1a–d Two patients with focal infiltrations of thoracic vertebrae by plasmacytoma (*arrows*). In **a** and **b**, short tau inversion recovery (STIR) images are shown before (**a**) and after (**b**) Endorem infusion. In **c** and **d**, STIR images are shown before (**c**) and after (**d**) Sinerem infusion. A reduced signal intensity of the normal bone marrow is shown after administration of both, Endorem and Sinerem, whereas focal tumors do not show any changes in signal intensity

Table 1 Patients with histologic subtype and stage of lymphoma, granulocyte colony stimulating factor (GCSF) treatment (+), or no GCSF treatment (–), and relative number of neoplastic cells estimated from iliac creast biopsies

Patient no.	Diagnosis	GCSF	Iliac crest biopsy
1	Plasmacytoma, IgG kappa stage IA	+	15% plasma cells multifocal
2	Plasmacytoma, IgG kappa stage IIIA	+	80% plasma cells multifocal
3	Plasmacytoma, IgA lambda stage IIIA	+	5% plasma cells multifocal
4	Plasmacytoma, IgA lambda stage IIIA	+	17% plasma cells multifocal
5	Lymphocytic lymphoma stage IVA	–	50% lymphocytes multifocal
6	Plasmacytoma, IgG lambda stage IIIA	+	70% plasma cells multifocal
7	Low-grade B-cell lymphoma stage IVA	–	20% lymphocytes multifocal
8	Plasmacytoma, IgA kappa stage IIIB	+	50% plasma cells diffuse
9	Low-grade B-cell lymphoma stageIV	–	Normal bone marrow, no tumor infiltration
10	Plasmacytoma, IgG kappa stage IIIA	+	5% plasma cells multifocal
11	Plasmacytoma, IgG kappa stage I	–	40% plasma cells multifocal
12	Plasmacytoma, IgG kappa stage III	–	70% plasma cells focal
13	Lymphocytic lymphoma stage IV	–	Normal bone marrow, no tumor infiltration
14	Plasmacytoma, IgG lambda stage I	–	20% plasma cells diffuse
15	Burkitt lymphoma stage IV	–	50% lymphocytes multifocal
16	Plasmacytoma, IgG kappa stage II	+	70% plasma cells diffuse
17	Lymphocytic lymphoma stage IV	–	50% lymphocytes multifocal
18	Plasmacytoma, IgG lambda stage IIIA	+	20% plasma cells diffuse

lar reconverted bone marrow in patients after GCSF treatment demonstrated a significantly stronger iron oxide enhancement as compared with the normocellular bone marrow in patients without GCSF treatment (Fig. 2).

Neoplastic bone marrow infiltration

Focal and multifocal bone marrow infiltration showed only a minor or no iron oxide uptake (Figs. 1, 3). On all pulse sequences, changes in tumor signal intensity pre- and post-contrast were not significant ($p>0.05$). The ΔSI(%) values did not correlate with the relative amount of tumor cells in the iliac crest biopsies ($p>0.05$). On STIR images mean ΔSI (%) values were significantly smaller in focal or multifocal lesions compared with normal hypercellular bone marrow after GCSF treatment ($p<0.05$; Fig. 2); thus, the reconverted hematopoietic bone marrow could be differentiated from multifocal tumor infiltration by the substantial decrease in signal in-

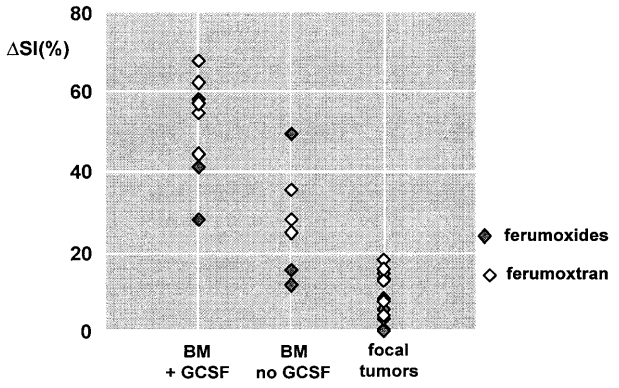

Fig. 2 Quantitative ΔSI(%) enhancement data of the bone marrow with and without granulocyte colony stimulating factor (GCSF) treatment as well as ΔSI(%) data of focal bone marrow infiltration by malignant lymphoma after infusion of either ferumoxide or ferumoxtran

Table 2 Bone marrow signal intensities (SI) before and after ferumoxides and ferumoxtran infusion with corresponding ΔSI(%) data, displayed as means and standard deviations. *TSE* turbo spin echo; *STIR* short tau inversion recovery

Pulse sequence		Ferumoxides	Ferumoxtran
T1 TSE	Pre-contrast	223.9±52.2	174.1±62.7
	Post-contrast	226.8±53.7	188.6±60.5
	ΔSI(%)	6.8±4.9	10.6±7.5
T2 TSE	Pre-contrast	93.6±22.5	101.8±24.8
	Post-contrast	68.6±22.2	73.8±24.5
	ΔSI(%)	13.7±9.0	28.6±5.6[a,b]
STIR	Pre-contrast	112.8±17.3	120.3±36.1
	Post-contrast	72.6±17.8	64.5±30.5
	ΔSI(%)	34.2±16.7[a,b]	46.9±16.1[a,b]

[a] Significant difference between pre- and post-contrast bone marrow signal intensities

[b] Significant differences between ferumoxides and ferumoxtran ($p<0.05$)

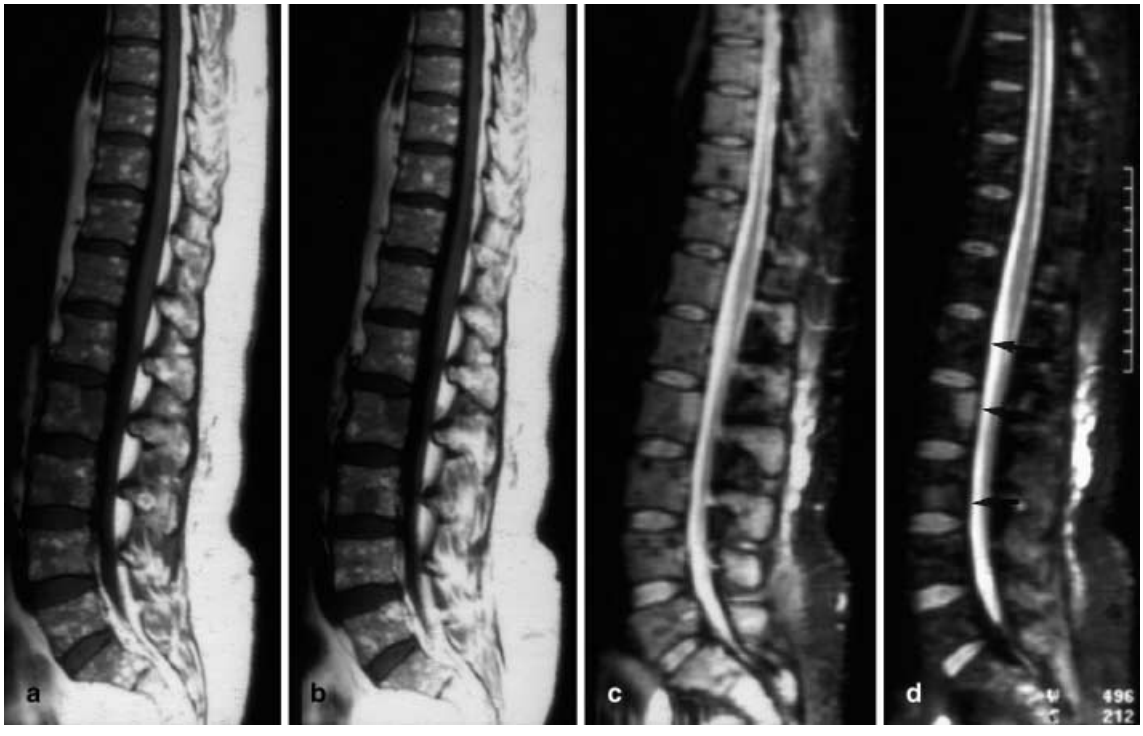

Fig. 3a–d A 42-year-old patient after recurrent chemotherapy and GCSF treatment with reconverted, hyperplastic hematopoietic marrow and multifocal bone marrow infiltration by lymphoma. Both, hematopoietic marrow and focal tumor infiltration, show a low signal intensity on **a** plain and **b** iron-oxide-enhanced T1-weighted images, as well as **c** an increased signal intensity on plain STIR images; however, **d** STIR images after iron oxide administration show a marked signal decrease of the hematopoietic marrow, whereas focal tumors (*arrows*) do not show any iron oxide uptake; thus, the tumor-to-bone marrow contrast increases substantially

tensity after iron oxide injection (Figs. 3, 4, 5). In addition, the contrast between normal bone marrow and focal tumors increased significantly after iron oxide infusion, and corresponding quantitative CNR data were higher after administration of ferumoxtran than after ferumoxides ($p<0.05$; Table 3).

Diffuse tumor infiltration showed a highly variable iron oxide uptake, which corresponded to the relative quantity of tumor cell infiltration. In patients with a relative amount of tumor cell infiltration of 50–70% the iron oxide enhancement of the bone marrow was minor with

Fig. 4a–d A 51-year-old patient with initially focal infiltration of Th 7 due to plasmacytoma. Status after local irradiation and concurrent cystic changes of the lesion (*arrows*). In addition, the patient underwent high dose chemotherapy and GCSF treatment. Magnetic resonance imaging after this treatment shows a diffuse hypointense bone marrow of the lower thoracic and lumbar spine on T1-weighted turbo spin-echo images **a** before and **b** after iron oxide administration. **c** Plain STIR images show multiple hyperintense foci in this area. **d** The STIR images after iron oxide infusion show that some areas of the bone marrow between these foci decrease in signal intensity, whereas the focal lesions remain unchanged (*arrowheads*). This lack of iron oxide uptake is indicative of multifocal neoplastic bone marrow infiltration and was confirmed by biopsy

Table 3 Bone marrow-to-tumor contrast-to-noise ratio (CNR) before and after infusion of ferumoxides and ferumoxtran, displayed as means and standard deviations

Pulse sequence		Ferumoxides	Ferumoxtran
T1 TSE	Pre-contrast	4.8±2.9	3.6±2.3
	Post-contrast	5.3±3.6	3.1±2.4
T2 TSE	Pre-contrast	5.1±2.2	3.3±2.4
	Post-contrast	5.7±2.7	4.5±2.4
STIR	Pre-contrast	8.1±1.9	7.4±2.9
	Post-contrast	10.2±2.7[a]	13.1±4.0[a]

[a] Significant difference between pre- and post-contrast CNR data ($p<0.05$)

a slightly, diffusely decreased signal intensity (Fig. 6). In patients with a minor amount of diffuse tumor cell infiltration (up to approximately 20%) the iron oxide uptake approximated that of normal hematopoietic bone marrow.

Discussion

The data presented in this study show that iron oxides may be used to target hematopoietic bone marrow, to increase the contrast between normal bone marrow and focal neoplastic infiltration, and to differentiate reconverted hyperplastic marrow and neoplasia. These results confirm previous observations of iron oxide uptake in the normal bone marrow and improved conspicuity of focal bone marrow lesions on ferumoxide-enhanced T2-weighted images, either noted incidentally [28, 29] or in a limited number of two volunteers and four patients [16].

The task of differentiating normal and neoplastic marrow with specific MR contrast agents has only recently been addressed, because with former conventional therapy regimes, unenhanced MR could easily differentiate tumor deposits and normal bone marrow when this had undergone a fatty conversion [7, 8, 9]. The diagnostic problem of differentiating reconverted hematopoietic marrow from bone marrow tumors occurred with the event of new high-dose chemotherapy regimes and new angiogenesis drugs, such as GCSF, which induced a re-

Fig. 5a–d A 41-year-old patient with malignant lymphoma. **a** The upper thoracic vertebrae show fatty marrow conversion after irradiation on plain and **b** iron-oxide-enhanced T1-weighted images. The lower thoracic vertebrae Th 7–10 and Th 2 and 5, however, show cellular marrow with low signal intensity on T1-weighted images and slightly increased signal intensity on plain STIR images (**c**, *arrowheads*). The bone marrow of these vertebrae shows a marked iron oxide uptake (**d**), indicating normal hematopoietic marrow

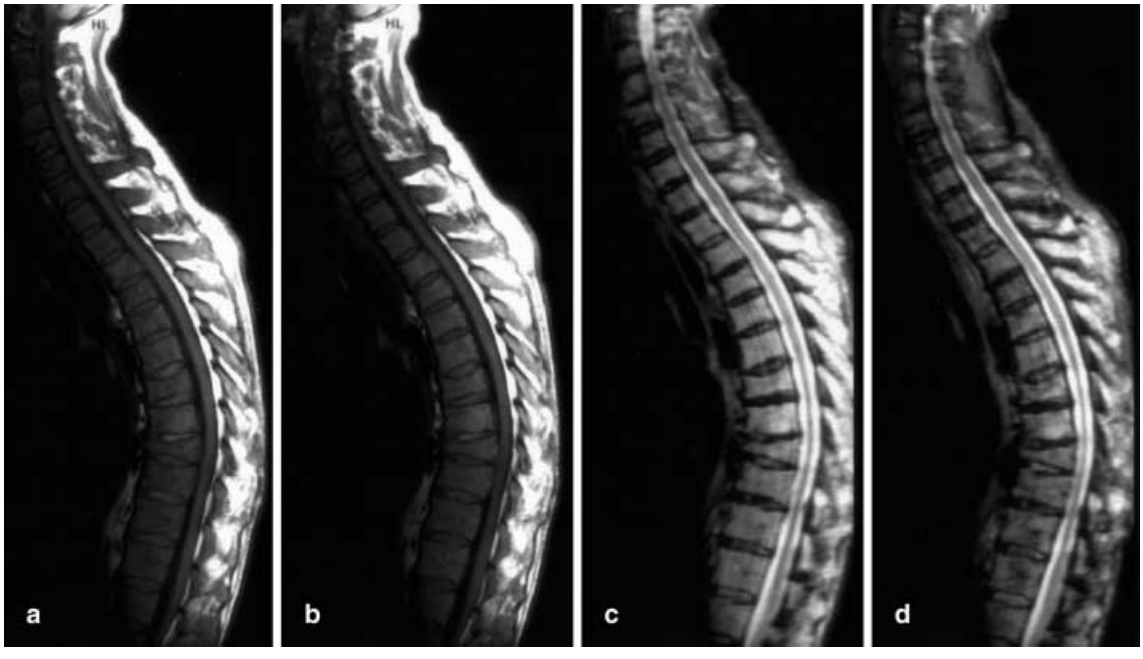

Fig. 6a–c A 57-year-old patient with plasmacytoma after chemotherapy and GCSF treatment. T1-weighted images **a** before and **b** after iron oxide infusion show a diffuse hypointense signal intensity of the bone marrow in all vertebrae and a pathologic fracture of Th 9. **c** Unenhanced STIR images show a diffuse hyperintense bone marrow, which shows only minimal changes in signal intensity after iron oxide infusion, indicative of diffuse tumor infiltration. Iliac crest biopsy revealed 80% tumor cells in the bone marrow

conversion of the fatty marrow and increased the cellularity of the normal bone marrow [30]. The increased cellularity of reconverted hematopoietic marrow caused changes in bone marrow MR signal intensities, which could not be differentiated from the increased cellularity due to neoplastic infiltration [30].

The pathophysiologic basis for the potential of ferumoxides and ferumoxtran to differentiate normal and neoplastic bone marrow is the distribution of RES cells in the bone marrow and their ability to phagocytose exogenous iron oxides. After chemotherapy, especially after GCSF treatment, reconversion from fatty to hematopoietic marrow occurs with an increasing number of all hematopoietic cell lines and RES cells [31, 32]. In bone marrow neoplasia, on the other hand, the hematopoietic marrow is replaced by tumor cells and the number of RES cells is substantially reduced [16]. Using conventional MRI, highly cellular reconverted hematopoietic marrow and tumor infiltration may not be differentiated [12, 14]. Iron-oxide-enhanced MRI, however, can differentiate these entities, because iron-oxide-targeted RES cells can be depicted in the reconverted hematopoietic marrow, but not in focal or multifocal tumor deposits.

The pharmacokinetics and physical properties of iron oxide particles provide an explanation for the observed changes in bone marrow signal intensities following intravenous administration: Although the majority of intravenously infused iron oxide particles are phagocytosed by liver and spleen, up to 5% is taken up by the bone marrow [16, 33]. These particles extravasate through the discontinuous endothelium of bone marrow sinusoids, are subsequently phagocytosed by bone marrow macrophages, and form clusters in secondary lysosomes of the macrophages [33, 34]. The small amount of iron oxides phagocytosed is sufficient to produce changes in T1- and T2-relaxation times of the bone marrow [16], which may be detected using standard MR pulse sequences [35]. The underlying physical mechanisms are dipolar interactions between superparamagnetic particles and surrounding protons with proton dephasing, either due to interactions of the outer-sphere type or due to a magnetic susceptibility effect [24, 36, 37].

The results of this study show that ferumoxtran may be better suited than ferumoxides to image bone marrow, because the negative bone marrow enhancement after administration of ferumoxtran is significantly higher [23, 38]. Ferumoxtran particles have a known higher bone marrow uptake as compared with ferumoxides, due to a four times smaller diameter and a 20 times higher endothelial permeability [23, 38]; thus, ferumoxtran particles are more likely to traverse the bone marrow sinusoids and to reach interstitial RES cells [23, 37]. Of note, we administered different doses of iron oxide particles with the two contrast agents, ferumoxides (15 µmol/kg) and ferumoxtran (30 µmol Fe/kg). These doses were recommended for clinical use. The underlying rationale was to test the potential of both agents to improve bone marrow tumor conspicuity in a clinical setting. It remains to be investigated whether doubling the contrast agent dose for ferumoxides would increase bone marrow uptake substantially; however, using a double dose for ferumoxides is not approved for clinical applications in humans, so the outcome would be of questionable significance.

Conclusions must be drawn to the scope and design of the study. Several limitations have to be considered: MRI cannot replace marrow biopsy, because the histopathologic subtype of lymphoma has to be defined, and because minimally diffuse, microscopic marrow involvement can be false negative with this imaging technique [39, 40]. As shown by this study, a low percentage of tumor cells which infiltrate bone marrow diffusely may not be detected with iron-oxide-enhanced MRI. On the other hand, routinely performed iliac crest biopsies cover only a small portion of the entire bone marrow and thus also provide a relatively high number of false-negative findings [2, 3, 40]. In a study by Hoane et al. in 98 patients with malignant lymphoma, up to one-third of the patients evaluated with routine blind iliac crest biopsies had occult marrow tumor detectable with MRI [40]. These authors concluded that optimal marrow evaluation should include both, biopsy and MRI [40].

In this study, MR examinations were started 45–60 min after iron oxide infusion, because previous investigators found a maximum bone marrow enhancement at this time interval, which, however, persisted for several days [16]. Since RES phagocytosis of iron oxides in the bone marrow is known to take several hours [34, 35, 36], further investigations have to address the sensitivity of late follow-up MRI studies.

All examinations described in this study were obtained on a high-field 1.5-T MR system. Since the susceptibility effect decreases with the square of the magnetic field strength, data have to be proven at lower field strength. At 0.5 T, Vande Berg and coworkers described significant changes in T1- and T2-relaxation times of the bone marrow after ferumoxide injection in a limited number of patients [16]; thus, results may also be reproducible on low magnetic field systems.

Of note, physiologic parameters of the bone marrow defined with gadolinium-based extracellular contrast agents are different from those defined with iron oxides [41]. Gadolinium-based extracellular contrast agents may define the vascularity of the bone marrow and differentiate normal and malignant bone marrow infiltration based on their perfusion patterns [42, 43, 44]; however, since the bone marrow blood volume is highly variable, both interindividually and within an individual [42], and since there is no histopathologic threshold of microvessel density that can differentiate normal and abnormal bone marrow, malignant tumors and highly vascularized reconverted hematopoietic marrow may show a broad overlap of gadopentetate enhancement patterns.

In conclusion, iron oxides may be used to improve the contrast between bone marrow tumors and normal hematopoietic marrow, and to differentiate NHL infiltration of the bone marrow and reconverted hematopoietic marrow after chemotherapy. Results encourage the continuing investigation of iron-oxide-enhanced MR imaging of the bone marrow.

Acknowledgement This work was supported by German research society (DFG) grant DA 529/1-1.

References

1. Durie B, Salmon SE (1975) A clinical staging system for multiple myeloma: correlation of measured myeloma cell mass with presenting clinical features, response to treatment and survival. Cancer 36:842–854
2. Coller BS, Chabner BA, Gralnick HR (1977) Frequencies and patterns of bone marrow involvement in non-Hodgkin's lymphomas: observations on the value of bilateral biopsies. Am J Hematol 3:105–119
3. Brunning R, Bloomfield C, McKenna R, Peterson L (1975) Bilateral trephine bone marrow biopsies in lymphoma and other neoplastic diseases. Ann Intern Med 82:365–366
4. Mariette X, Zagdanski A, Guermazi A, Bergor C, Arnould A, Frija J, Brouet JC, Fermand JP (1999) Prognostic value of vertebral lesions detected by MRI in patients with stage I multiple myeloma. Br J Haematol 104:723–729
5. Kusumoto S, Jinnai I, Itoh K, Kaeai N, Sakata T, Matsuda A, Tominaga K, Murohashi I, Bessho M, Harashima K, Heshiki A (1997) MRI patterns in patients with multiple myeloma. Br J Haematol 99:649–655
6. Vande Berg B, Lecouvet F, Michaux L, Labaisse M, Malghem J, Jamaert J, Maldague BE, Ferrant A, Michaux JL (1996) Stage I multiple myeloma: value of MRI of the bone marrow in the determination of prognosis. Radiology 201:243–246
7. Kricun M (1985) Red-yellow marrow conversion: its effect on the location of some solitary bone lesions. Skeletal Radiol 14:10–19
8. Moore S, Dawson K (1990) Red and yellow marrow in the femur: age related changes in appearance at MRI. Radiology 175:219–223
9. Ricci C, Cova M, Kang Y, Yang A, Rahmouni A, Scott W, Zerhouni E (1990) Normal age related patterns of cellular and fatty bone marrow distribution in the axial skeletton: MR imaging study. Radiology 177:83–88
10. Vogler J, Murphy W (1988) Bone marrow imaging. Radiology 168:679–693
11. Flickinger F, Salahattin S (1994) Bone marrow MRI: techniques and accuracy for detecting breast cancer metastases. Magn Reson Imaging 12:829–835
12. Layer G, Sander W, Träber F, Block W, Ko Y, Ziske CG, König R, Vahlensiek M, Schild HH (2000) Diagnostic problems of MRI in studying the effect of G-CSF therapy in bone marrow of patients with malignoma. Radiologe 40:710–715
13. Vanel D, Missenard G, Le Cesne A, Guinebretiere J (1997) Red marrow colonization induced by growth factors mimicking an increase in tumor volume during preoperative chemotherapy; MR study. J Comput Assist Tomogr 21:529–531
14. Fletcher B, Wall J, Soheil L (1993) Effect of hematopoietic growth factors on MR images of bone marrow in children undergoing chemotherapy. Radiology 189:745–751
15. Hansen B, Jensen K, Larsen V, Johnsen HE, Nielsen H, Karle H, Henriksen O (1995) Short-term stimulation with myeloid growth factors expands bone marrow hematopoiesis. A magnetic resonance spectroscopy study. Ugeskr Laeger 157:6265–6269
16. Vande Berg B, Lecouvet F, Kanku J, Jamaert J, Van Beers BE, Maldague B, Malghem J (1999) Ferumoxides-enhanced quantitative magnetic resonance imaging of the normal and abnormal bone marrow: preliminary assessment. J Magn Reson Imaging 9:322–328
17. Seneterre E, Weissleder R, Jaramillo D, Reimer P, Lee AS, Brady TJ, Wittenberg J (1991) Bone marrow: ultrasmall superparamagnetic iron oxide for MR imaging. Radiology 179:529–533
18. Weissleder R. (1994) Liver MR imaging with iron oxides: toward consensus and clinical practice. Radiology 193:593–595
19. Jung CW (1995) Surface properties of superparamagnetic iron oxide MR contrast agents: ferumoxides, ferumoxtran, ferumoxsil. Magn Res Imaging 13:675–691
20. Weissleder R, Stark D, Engelstad B, Bacon B, Compton C (1989) Superparamagnetic iron oxide: pharmacokinetics and toxicity. Am J Roentgenol 152:167–173
21. Stark D, Weissleder R, Elizondo G, Hahn PF, Saini S, Todd LE, Wittenberg J, Ferrucci JT (1988) Superparamagnetic iron oxide: clinical application as a contrast agent for MR imaging of the liver. Radiology 168:297–301
22. Pouliquen D, Perroud H, Calza F, Jallet P, Le Jeune J (1992) Investigation of magnetic properties of iron oxide nanoparticles used as contrast agents for MRI. Magn Reson Med 24:75–84
23. Weissleder R, Elizondo G, Wittenberg J, Rabito C, Bengele H, Josephson L (1990) Ultrasmall superparamagnetic iron oxide: characterization of a new class of contrast agents for MR imaging. Radiology 175:489–493
24. Chambon C, Clement O, Le Blanche A, Schouman-Claeys E, Frija G (1993) Superparamagnetic iron oxides as positive contrast agents: in vitro and in vivo evidence. Magn Reson Imaging 11:509–519
25. Vassallo P, Matei C, Heston W, McLachlan S, Koutcher J, Castellino R (1994) AMI-227-enhanced MR lymphography: utility for differentiating reactive from tumor-bearing lymph nodes. Radiology 193:501–506
26. Stillman A, Wilke N, Li D, Haacke M, McLachlan S (1996) Ultrasmall iron oxide to enhance MRA of the renal and coronary arteries: studies in human patients. J Comput Assist Tomogr 20:51–55
27. Frank H, Weissleder R, Brady TB (1994) Enhancement of MR angiography with iron oxide: preliminary studies in whole-blood phantom and in animals. AJR 162:209–213
28. Saini S, Stark D, Hahn P, Wittenberg J, Brady T, Ferruci J (1987) Ferrite particles: a superparamagnetic MR contrast agent for the reticuloendothelial system. Radiology 162:211–216
29. Gandon Y, Heautot J, Brunet F, Guyader D, Deugnier Y, Carsin M (1991) Superparamagnetic iron oxide: clinical time response study. Eur J Radiol 12:195–200
30. Ryan S, Weinberger E, White K, Shaw DW, Patterson K, Nazar-Stewart V, Miser J (1995) MR imaging of bone marrow in children with osteosarcoma: effect of granulocyte colony-stimulating factor. Am J Roentgenol 165:915–920

31. Nguyen Y (1994) Granulocyte colony stimulating factor. J Fla Med Assoc 81:467–469
32. Lieschke G, Burgess A (1992) Granulocyte colony-stimulating factor and granulocyte-macrophage colony-stimulating factor. N Engl J Med 327:28–35
33. Daldrup H, Link T, Blasius S et al. (1999) Monitoring radiation induced changes in bone marrow histopathology with ultra-small superparamagnetic iron oxide (USPIO)-enhanced MRI. J Magn Reson Imaging 9:643–652
34. Daldrup-Link H, Reinlaender C, Link T, Richter K-J, Koenemann S, Rummeny EJ (2001) Value of SPIO for MRI of the bone marrow before and after total body irradiation (TBI): initial investigations in an animal model. Fortschr Roentgenstr 173:547–553
35. Hundt W, Petsch R, Helmberger T, Reiser M (2000) Effect of superparamagnetic iron oxide on bone marrow. Eur Radiol 10:1459–1500
36. Guimaraes R, Clement O, Bittoun J, Carnot F, Frija G (1993) MR lymphography with superparamagnetic iron nanoparticles in rats: pathologic basis for contrast enhancement. AJR 162:201–207
37. Muller R, Gillis P, Moiny F, Roch A (1991) Transverse relaxivity of particulate MRI contrast media: from theories to experiments. Magn Reson Med 22:178–182
38. Bankstrom P, DeBruyn P (1974) The permeability to carbon of the sinusoidal lining cells of the embryonic rat liver and rat bone marrow. Am J Anat 141:281–290
39. Richards M, Webb J, Jewell SE, Amess JA, Lister TA (1988) Low field strength magnetic resonance imaging of bone marrow in patients with malignant lymphoma. Br J Cancer 57:412–415
40. Hoane B, Shields A, Porter BA, Shulmann HM (1991) Detection of lymphomatous bone marrow involvement with magnetic resonance imaging. Blood 78:728–738
41. Hawighorst H, Libicher M, Knopp M, Moehler T, Kauffmann G, van Kaick G (1999) Evaluation of angiogenesis and perfusion of bone marrow lesions: role of semiquantitative and quantitative MRI. J Magn Reson Imaging 10:286–294
42. Baur A, Stäbler A, Bartl R, Lamerz R, Scheidler J, Reiser M (1997) MRI gadolinium enhancement of bone marrow: age-related changes in normals and in diffuse neoplastic infiltration. Skeletal Radiol 26:414–418
43. Bollow M, Knauf W, Korfel A, Taupitz M, Schilling A, Wolf K-J, Hamm B (1997) Initial experience with dynamic MR imaging in evaluation of normal bone marrow versus malignant bone marrow infiltration in humans. J Magn Reson Imaging 7:241–250
44. Vanel D, Dromain C, Tardivon A (2000) MRI of bone marrow disorders Eur Radiol 10:224–229